

# Time delay controversy on QSO 0957+561 not yet decided

J. Pelt<sup>1</sup>, W. Hoff<sup>2</sup>, R. Kayser<sup>2</sup>, S. Refsdal<sup>2</sup>, and T. Schramm<sup>2</sup>

<sup>1</sup> Tartu Astrophysical Observatory, EE2444 Tõravere Estonia

<sup>2</sup> Hamburger Sternwarte, Gojenbergsweg 112, D-21029 Hamburg-Bergedorf, Germany

received ;date; ; accepted ;date;

**Abstract.** We present a new analysis of previously published optical and radio data sets of the gravitationally lensed quasar 0957+561 A,B with the aim of determining the time delay between its two images. We use a non-parametric estimate of the dispersion of the combined data set where, however, we only make use of alternating neighbours in order to avoid windowing effects. From the optical data a time delay of  $(415 \pm 32)$  days and from the radio data a delay of  $(409 \pm 23)$  days is suggested. We demonstrate a considerable sensitivity of different delay estimation procedures against the removal of only a few observational data points or against smoothing or detrending of the original data sets. The radio data give us formally a slightly more precise value for the time delay than the optical data. Also, due to the lack of windowing effects, the result obtained for the radio data can be considered as somewhat more reliable than the delay determined from the optical data.

**Key words:** Methods: statistical – time series analysis – Quasars: 0957+561A,B – gravitational lensing – time delay

## 1. Introduction

The time delay between the images of a gravitationally lensed object is of great astrophysical interest since it may be used to determine the Hubble parameter as well as the mass of the lens (Refsdal 1964a, 1964b, Borgeest 1986, Falco et al. 1991b). The double quasar 0957+561 A,B (Walsh et al. 1979, Young 1980, Falco 1992) is up to now the only gravitational lens system for which serious attempts have been made to determine the time delay  $\tau$  between its images. However, the results are still controversial, with suggested time delays of between 376 and 657 days (Florentin-Nielsen 1984, Schild & Cholfin 1986, Gondhalekar 1986, Gorenstein et al. 1988, Lehár

et al. 1989, Vanderriest 1989, Schild 1990, Falco et al. 1991a, Lehár et al. 1992, Roberts et al. 1991, Press et al. 1992a, 1992b, Beskin & Oknyanskij 1992). Using an elaborate statistical method (see Rybicki et al. 1992) Press et al. (1992a, below PRHa), recently obtained a value of  $(536 \pm 12)$  days from the optical lightcurve, which is seemingly in good agreement with the value obtained from the radio data by the same authors (Press et al. 1992b, below PRHb). They conclude that “delays less than about 475 days are strongly excluded”. It is also often claimed (Lehár 1992, Roberts et al. 1991, PRHb) that the radio data decisively exclude a delay of around 415 days, a value favoured by other authors (Vanderriest et al. 1989, Schild 1990).

The time delay obtained by PRHa is quite close to 1.5 years, a value for which windowing effects due to the uneven sampling of the optical data are expected to be strongest (Vanderriest et al. 1992).

We here present results of a careful re-analysis of the same data sets as used in PRHa and PRHb using simple explorative type statistical methods. The main emphasis of our work is the evaluation of two competing hypothetical time delays: 415 and 536 days.

For the combined data set generated from the data of image A and the data of image B, time shifted by  $\tau$ , we basically estimate the dispersion  $D^2$  of the scatter around the unknown mean curve. The true time delay between the images should then show up as a minimum in the dispersion spectrum  $D^2(\tau)$ . It is our aim to determine the dispersion of the combined data due to the alternation between the two light curves, and not the dispersion within each lightcurve. In order to avoid strong windowing effects we therefore take into account only alternating neighbouring pairs in the combined data set, i.e. only pairs where one point is from A and the other one from B, respectively. It should be noted that for  $\tau = (n + 0.5)$  years (where  $n$  is integer) the dispersion  $D^2(\tau)$  would otherwise be strongly dominated by the inner dispersion of the two original light curves, naturally leading to pronounced minima.

In Section 2 of the paper we introduce the basic statistical techniques used. In Section 3 we present the results

*Send offprint requests to:* R. Kayser

of a detailed analysis of the light curves of the double quasar 0957+561 A,B. We here use the same data sets as PRHa and PRHb to allow a comparison of the results and to understand the problems leading to the different results. In the concluding part we try to summarize the work done on time delay estimation up to now and to delineate some inner difficulties of the problem under study. Technical details of the nonparametric dispersion estimation are treated in the Appendix.

## 2. Data analysis methods

### 2.1. The optimal prediction

In the papers PRHa, PRHb and Rybicki et al. (1992) a rather complex procedure for an optimal interpolation of the lightcurves was developed. The procedure itself is practically the same as used in geophysical research under the name of *kriging* (Cabrera et al. 1990). The use of sound statistical arguments and validation of the results by Monte-Carlo simulations allowed the authors to draw conclusions on the probable time delay with a (formally) high level of confidence. Since our analysis did not fully confirm these results, we reimplemented the procedures used in PRHa and PRHb and used some simple procedures to check the inner consistency of the results. We started from a very simple computation of the num-

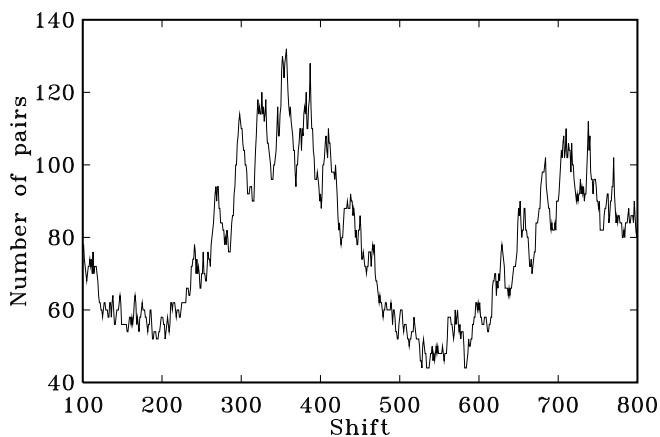


**Fig. 1.** Window function for optical data

ber of mixed data pairs in the combined sequence (data set B shifted by  $\tau$  coalesced with data set A). In Fig. 1 the number of neighbouring data pairs of mixed type (one from data set A, one from data set B) is plotted against the trial time delays. This simple statistic measures well the total overlap between the two data sets for different shifts in time of the B component. Inside of the range of probable delays quoted in PRHa two strong minima at  $\tau = 527$  days,  $N_{A,B} = 43$  and at  $\tau = 535$  days,  $N_{A,B} = 43$  are found. There is a strong similarity between the win-

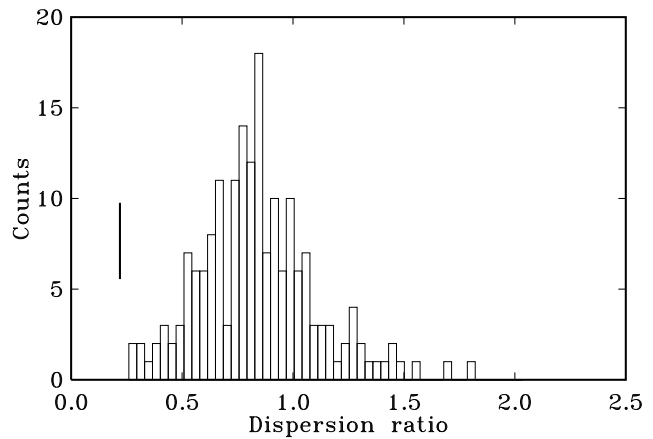


**Fig. 2.** Distribution of dispersion ratios for artificial light curves generated by Monte-Carlo method. The value obtained from the original optical data is marked with a dash.

dow function plot in PRHa and our simple statistic. It is quite obvious (and was noticed also by PRHa) that the coincidence of minima in the window function and in the  $\chi^2$  spectrum in PRHa is a rather serious signal about the complexity of problems one encounters with the lightcurves of QSO 0957+561.

After reimplementation of the PRHa procedures we carried out the following simple experiment. We divided the data points of the combined data set (computed with  $\tau = 536$  days) into two subsets: relevant and irrelevant. Into the first subset we included observations which had at least one nearest neighbour from alternate original data sets, and into the second subset we included observations for which both neighbours had the same origin as the data point under consideration. After computation of the optimally approximated (predicted) values for all data points, we were now able to compute separately prediction errors for relevant and irrelevant observational points. *We found that the dispersion for relevant points was by a factor of five larger than that for irrelevant points.*

This result lead us to another interesting test. We repeated Monte-Carlo simulation runs with different time delay values exactly as described in PRHa and used our data set subdivision procedure for each of the generated artificial data sets. In Fig. 2 the resulting distribution of dispersion ratios is shown. The mean ratio is slightly less than unity. This fact can be explained in the following way: the overlap regions for the two original data sets are populated in the mean two times more densely than regions where only one data set is seen. For the sparsely populated regions there is a tendency for the optimal prediction procedure to put the prediction curve through the observed points and consequently in these regions the dispersion for prediction errors is as a rule less than for overlapped regions. However, as can be seen from the distribution di-

agram, the typical decrease is by far not as severe as for the original data set (marked in Fig. 2).

The conclusion is discouraging: the Monte-Carlo procedure proposed in PRHa, which was considered as *experimentum crucis* for their time delay computations does not model the actual data set at hand, but *it proves only that for data sets with certain regular statistical properties their procedure works quite well*. The real data set is unfortunately more complex, this is probably caused by microlensing.

Our negative experience with the optimal prediction procedure lead us to the conclusion that to understand all the intricacies involved with the actual observations we must seek some extremely simple statistics whose use is not shadowed by the complexities of the mathematical procedures involved. Our aim was not so much to prove that one or another delay value is right or wrong, but to understand how the different values are “cooked” from the data set.

## 2.2. Use of nonparametric dispersion estimates for shift analysis

Let  $A_i = g(t_i) + \epsilon_A(t_i)$ ,  $i = 1, 2, \dots, N_A$  and  $B_j = (g(t_j + \tau) - a) + \epsilon_B(t_j)$ ,  $j = 1, 2, \dots, N_B$  be two time series which are different measurements of the original light curve  $g(t)$ . It is assumed that for channel B the observations  $B_j$  are amplified with an unknown amplification ratio  $a$ . Observed values contain also observational errors  $\epsilon_A(t_i)$ ,  $\epsilon_B(t_j)$  for which we may have certain dispersion estimates  $\delta_A^2(t_i)$ ,  $\delta_B^2(t_j)$  or corresponding statistical weights  $W_A(t_i)$ ,  $W_B(t_j)$ . Our task is to estimate the time shift parameter  $\tau$  from observed time series.

For every fixed set of values  $\tau, a$  we can construct a combined data set from both observed series

$$C_k(t_k) = \begin{cases} A_i, & \text{if } t_k = t_i, \\ B_j + a, & \text{if } t_k = t_j + \tau \end{cases} \quad (1)$$

and estimate its dispersion  $D^2(\tau, a)$  with the simple nonparametric method described in the Appendix. The *dispersion spectrum* is now defined as:

$$D^2(\tau) = \min_a D^2(\tau, a). \quad (2)$$

Statistical weights can be introduced into our scheme by using the usual combined weights for every pair of observations. If the statistical weight of channel A is  $W_i$  and that of channel B is  $W_j$  then the dispersion for the difference  $A_i - (B_j + a)$  is equal to

$$\frac{1}{W_i} + \frac{1}{W_j}, \quad (3)$$

and the squared difference of the two observations must be consequently included with weights

$$W_{i,j} = \frac{W_i W_j}{W_i + W_j}. \quad (4)$$

A correct normalization is obtained by dividing the corresponding sums of squared differences by the total sum of weights.

By choosing different selection windows (see Appendix) we can now compute different statistics and compute corresponding dispersion spectra. In several numerical experiments we tried to understand the behaviour of many different variants depending on features in the data sets at hand. However, to present our results we use only one, and by the way the simplest algorithm: only neighbouring data points are considered as near enough, to be included in the cross-sums. We even do not specify an upper limit  $\delta$  for a maximum allowed time separation between two sequential points. This approach allows us to avoid *any free parameters* in our procedures, and makes the calculations simple enough to be well reproduced by other researchers.

Correspondingly, we use in the following analysis only two simple statistics. The first one

$$D_{\text{all}}^2 = \min_a \frac{\sum_{k=1}^{K-1} W_{k,k+1} (C_{k+1} - C_k)^2}{2 \sum_{k=1}^{K-1} W_{k,k+1}} \quad (5)$$

measures the general dispersion of the combined data set. The second statistic

$$D_{\text{A,B}}^2 = \min_a \frac{\sum_{k=1}^{K-1} W_{k,k+1} G_k (C_{k+1} - C_k)^2}{2 \sum_{k=1}^{K-1} W_{k,k+1} G_k} \quad (6)$$

where  $G_k = 1$  only when  $C_{k+1}$  and  $C_k$  are from different data sets and  $G_k = 0$  otherwise, measures the dispersion in the overlap areas of the combined light curve.

## 2.3. Computation of error bars for time delays

To get an idea about error bars for the minima in the dispersion spectra we used a simple bootstrap procedure. We applied a 7-point median filter to smooth the combined light curve and reshuffled the corresponding residuals 1000 times to generate bootstrap samples. The full procedure turned out to be not very dependent on the median filter length, we therefore present only results for the particular value of 7.

It must be stressed that the somewhat arbitrary value for the filter length was used only to estimate mean square errors of the computed values of the minima, the minima themselves do not depend on any prechosen numerical constant.

It is possible to get much more narrow limits to the computed shift estimates by using longer smoothing filters, but we wanted to be as conservative as possible.

## 2.4. Influential data segments

To demonstrate the effect of removing short segments of data from the analysis we used the following simple procedure. For any starting index value  $l$  in the row of ob-

servations, for any skip length  $m$  and for any pair of hypothetical shift values  $S_1, S_2$  which are interesting for us we can compute the statistic (*gain* of hypothesis  $\tau = S_1$  against  $\tau = S_2$ )

$$I(l, m, S_1, S_2) = D_{A,B}^2(l, m, S_1) - D_{A,B}^2(l, m, S_2) \quad (7)$$

where the dispersions are computed for data sets with skips (start of data skip from  $l$ , length of skipped subset  $m$  points). In various experiments we used different skipping schemes: sometimes we skipped observing points for both channels, sometimes only from one channel. The statistic  $I(l, m, S_1, S_2)$  allowed us to compare the influence of skipped values for two different hypothetical time delays. Maxima and minima in  $I(l, m, S_1, S_2)$  indicate skips which favor hypothesis  $S_2$  and hypothesis  $S_1$ , respectively.

This kind of approach is quite common in standard regression analysis where robustness of the predicted curve is tested against removal of a small number of observed values (outliers). In our case we assume that the correct estimate for the time delay should not depend strongly on a small number of observations. If it does, we conclude that some of the data points are real outliers, or that the available data sets do not contain enough information to discriminate between the two hypotheses.

### 3. Analysis of observed data sets

#### 3.1. Optical data

We used the same data as PRHa, i.e. the optical data published by Vanderriest et al. (1989). The  $D_{\text{all}}^2$  (Eq. 5) and  $D_{A,B}^2$  (Eq. 6) statistics for the original optical data set are depicted in Fig. 3. The strongest local minima in the  $D_{A,B}^2$  spectrum is at a shift of 525 days and bootstrap calculations give us a standard error value of 42 days, so that our result is in good agreement with the value given in PRHa. It is interesting to note that the mean shift for the bootstrap trials occurred to be biased to a shift of 534 days. There is an additional depression around 415 days which is, however, somewhat weaker than the main “peak”. It is important to note that the  $D_{A,B}^2$  spectrum stays *everywhere* well above the  $D_{\text{all}}^2$  spectrum, i.e. the dispersion in the overlap region is systematically higher than in the intervening regions. We therefore conclude that there must be a certain amount of additional mutual variability between two light curves (maybe due to microlensing), so that the model of shifted but otherwise similar images, which has been used here and in PRHa, is oversimplified.

To get an idea about the form of the real depression in the dispersion spectra we proceed with a simple numerical experiment. We combined the A and B datasets with the best shift and the best  $a$  value, filtered the combined data set with a 7-point median filter, and decompose the filtered set back into two subsets. The spectra for the real data set and for the artificial data set (with a delay of 536 days) are given in Fig. 4. The spectrum

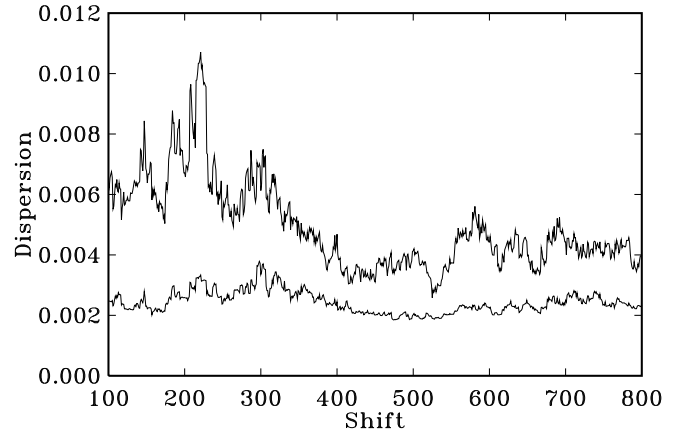


**Fig. 3.** Dispersion spectra for original optical data. Upper curve is  $D_{A,B}^2(\tau)$ , lower curve is  $D_{\text{all}}^2(\tau)$

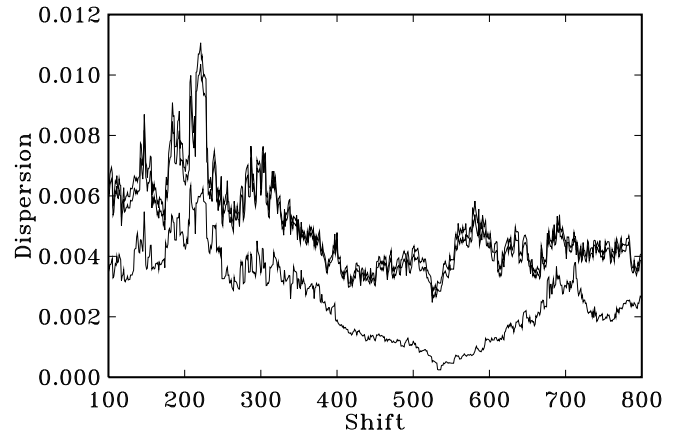


**Fig. 4.** Dispersion spectra for original and artificial data sets. The two upper curves are  $D_{A,B}^2(\tau) \pm \mathbf{D}(\tau)^{1/2}$  for the original data, the lower curve is  $D_{A,B}^2(\tau)$  for the artificial data

for the real data set is depicted in the two nearby curves. The upper curve is the dispersion spectrum *plus* the estimated subsampling error for the particular shift value and the lower curve is the dispersion spectrum *minus* the subsampling error estimate. Thus, the difference between the two curves demonstrates the uncertainty due to the subsampling. The minimum value in the spectrum for the artificial set (which is  $D_{\text{trend}}^2$  if we use the notation from the Appendix, see Eq. (A9)) is comparable to the largest difference between the upper and the lower limit for the original spectra. It is therefore clear that our dispersion estimation scheme works here (at least in the region of the main minimum) nearly optimally. It can be seen that the “line profiles” of the real and the artificial spectra differ significantly. The feature in the real spectrum is more fluctuation like than the wide and systematic depression in the artificial spectrum.

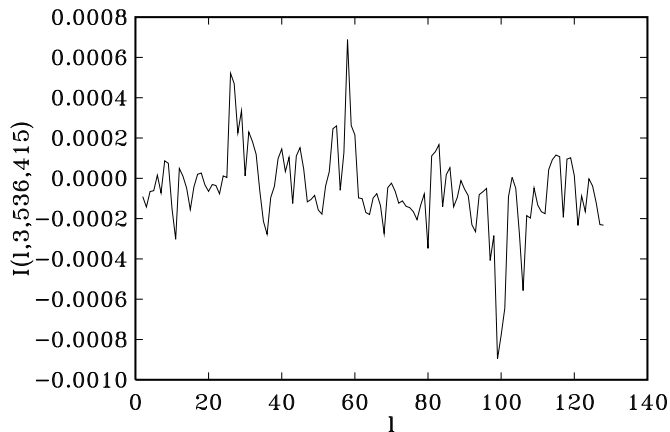


**Fig. 5.** Gain of hypothesis  $\tau = 536$  days against hypothesis  $\tau = 415$  days for different locations of the three point gap in the original data set

We then investigated the robustness of our first solution against skipping short segments from both light curves. The strong motivation to do this kind of analysis stems from the remark of PRHa that the “feature at epoch 6200” can bias estimation of the shift value towards 415 days.

In Fig. 5 the results of a typical sensitivity analysis are shown. The gain  $I(l, 3, 536, 415)$  (Eq. 7) of hypothesis  $\tau = 536$  days against  $\tau = 415$  days is plotted against the starting index of a three point skip in the original data set. In Fig. 6 the corresponding spectra are plotted: one with the most favorable (for hypothesis  $\tau = 536$  days, minimum at  $l = 99$ ) skip, and one with the most unfavourable (maximum at  $l = 58$ ). It is seen that the feature in the region of 536 days undergoes a rather dramatic change, whereas the feature around 415 days remains relatively stable. By skipping only *three consecutive time points* (the A and B channels are observed simultaneously) we can strongly emphasize the 536 feature, or remove it completely! There is no need to say that for longer gaps the effect of skips is even more drastic.

From these experiments we concluded that it is reasonable to investigate the high frequency behaviour of the optical data sets. Since our investigation is of explorative type, we postulated freely (at least for the moment) that both light curves are corrupted by independent low frequency components (which can be physically interpreted as microlensing). We assumed that these components can be modeled by low degree polynomials. In Figs. 7 and 8 the  $D_{A,B}^2$  spectra for data sets which were obtained by removing polynomial trends with degrees 1 – 9 from the original data sets are shown. The feature around 415 days is much stronger than the feature around 536 days for degrees 1,3,5,6,7,8,9. For degrees 2 and 4 (see Fig. 7) the minima for both hypothetical shifts are comparable. It is evident that starting from degree 5 the behaviour of dis-

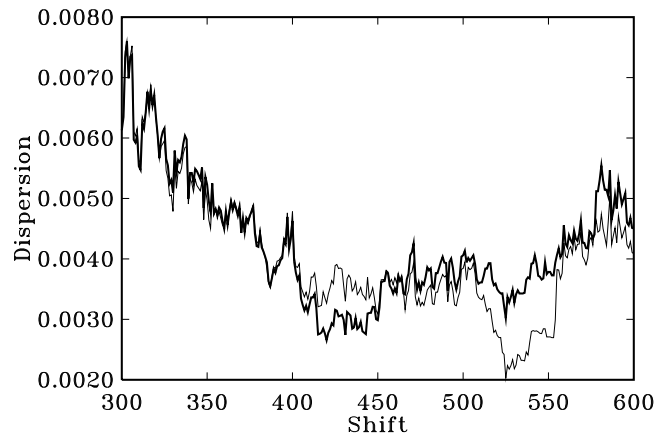


**Fig. 6.** Comparison of the two dispersion spectra obtained by different skips from the data sets. The three point gaps started from  $l = 58$  for the bold curve and from  $l = 99$  for the normal curve

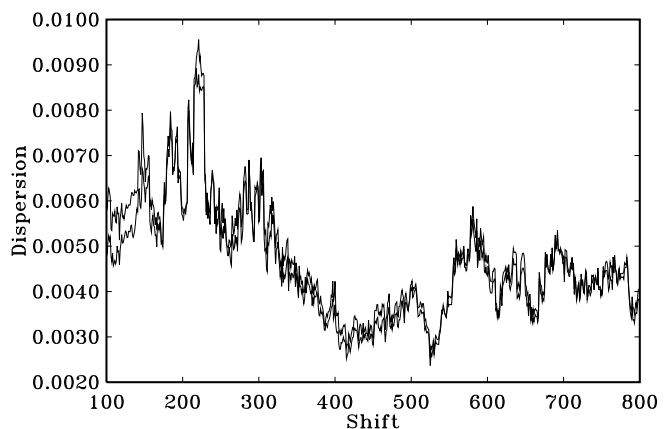


**Fig. 7.** Dispersion spectra for the detrended data sets. On the plot the results for degrees 2 and 4 are depicted.

ersion spectra is quite similar. For our further presentations we arbitrarily choose polynomials with degree 9 and in the following discussion we use as detrended data sets the corresponding least squares fit residuals. The computations with other degrees (from 5 to 8) gave essentially the same results. In Fig. 9 the  $D_{\text{all}}^2$  and  $D_{A,B}^2$  spectra for the detrended data are depicted.

It is worth to note that the minimum of  $D_{A,B}^2$  now nearly coincides with the value of  $D_{\text{all}}^2$  for the same shift. Correspondingly the dispersion for the overlap areas and for the intervening areas are nearly the same for the best shift! *The excess dispersion between the two light curves, which is probably due to microlensing, is removed.* At least from this point of view the  $\tau = 415$  days solution is much more consistent than the solution with  $\tau = 536$  days.

We then repeated our experiment with the artificial data set. In Fig. 10 the overall correspondence between

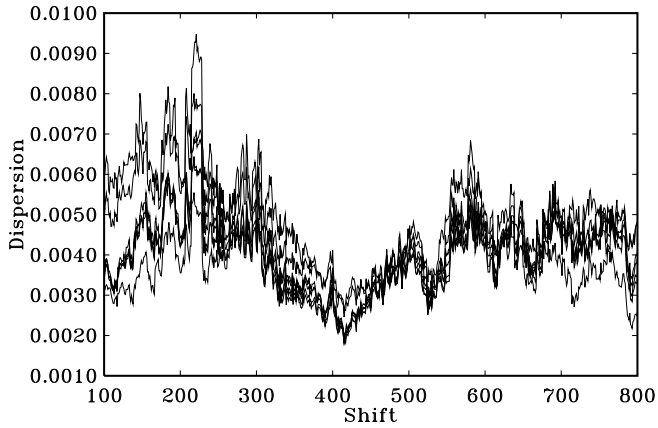


**Fig. 8.** Dispersion spectra for the detrended data sets. On the plot the results for degrees 1, 3, 5, 6, 7, 8, 9 are depicted.

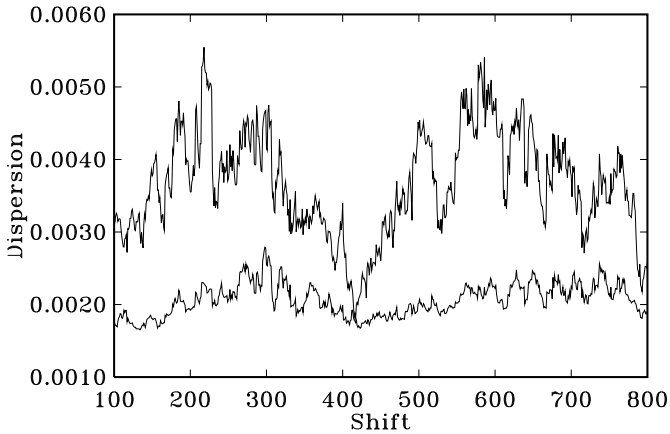


**Fig. 9.** Dispersion spectra for the data sets detrended by polynomials of degree 9. The upper curve is  $D_{A,B}^2(\tau)$  and the lower curve is  $D_{all}^2(\tau)$ .

the two spectra is striking. It seems, however, that the exact value of 415 days for the very narrow dip of the real spectrum can be slightly out of place, because it is “cooked” by high frequency local fluctuation just on the bottom of the feature.

The sensitivity analysis for the detrended data sets is also revealing. In Figs. 11 and 12 it can be seen that the feature around 536 days can be amplified significantly or can be removed nearly completely by skipping three consecutive observing nights from the original data sets. On the other hand the depression around 415 is rather stable.

The bootstrap procedure gives us for the detrended data a standard error of  $\pm 32$  days for the alternative solution of 415 days. The distribution of 1000 trials is depicted in Fig. 13.

There are two competing values for the time delay, both of which we were able to derive from optical data

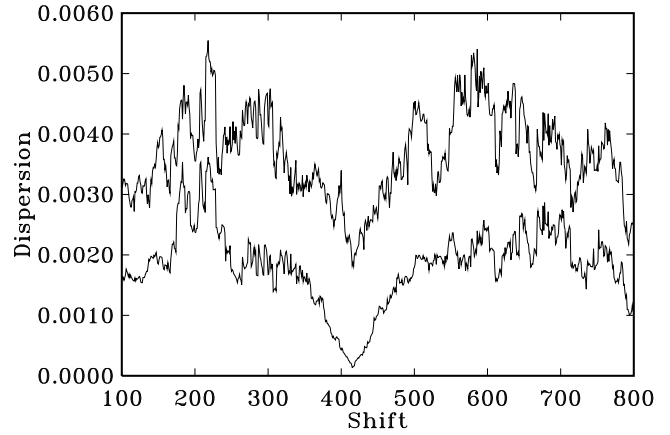


**Fig. 10.** Dispersion spectra for detrended (with 9-degree polynomial) and artificial data sets. The upper curve is  $D_{A,B}^2(\tau)$  for detrended data set and the lower curve is  $D_{A,B}^2(\tau)$  for artificial data set.

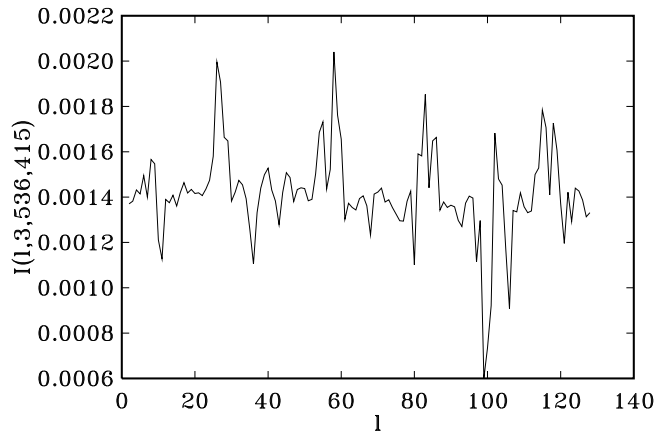


**Fig. 11.** Gain for hypothesis  $\tau = 536$  against hypothesis  $\tau = 415$  for detrended data sets with three consecutive data points removed.

using exactly the same techniques. We hoped that the analysis of the radio data could have given us clues as to which of them should be preferred.

### 3.2. Radio data

We used the radio data published by Lehár et al. (1992) exactly in the manner they were used in PRHb. The observations marked in PRHb by an asterisk were skipped and the other observed values were transformed to logarithmic scale. The  $D_{all}^2$  and  $D_{A,B}^2$  spectra (Eqs. 5 and 6) for the radio data are depicted in Fig. 14. The total minimum at  $(533 \pm 40)$  days (error bars from bootstrapping) is again in very good agreement with the result of PRHb. This coincidence is so good that one may well be inclined to drop the  $\tau = 415$  day hypothesis completely. The plot

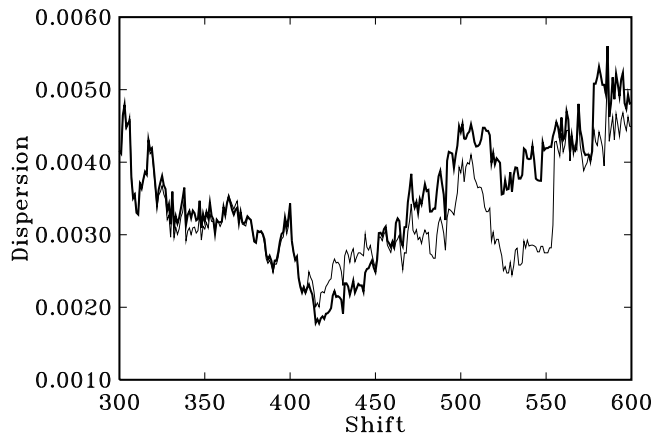


**Fig. 12.** Dispersion spectra for the two skipping schemes with maximum contrast between two hypotheses. The three point gaps started from  $l = 58$  for the bold curve and from  $l = 99$  for the normal curve.

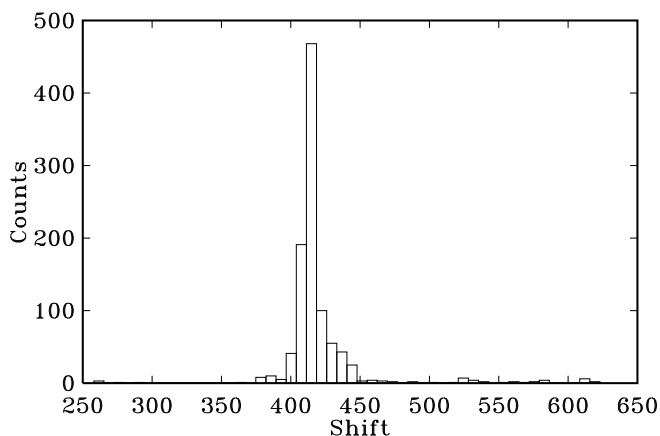


**Fig. 13.** Distribution of shifts for the bootstrap simulations for the optical data.

of two light curves with appropriate shift and parameter  $a$  (Fig. 15) fits well into this picture.

Nonetheless, we applied to the radio data some of the tests already used for the optical data. We first repeated the experiments with artificial data sets generated from the combined original data sets by 7-point median filtering. In Fig. 16 the plot of the original and the artificial spectra are shown. The results are not very convincing, neither *pro* nor *contra*. However, it seems that the artificial spectrum (with  $\tau = 533$  days) has a slightly more pronounced minimum.

We then experimented with various skipping schemes, to look how stable our results are against removal of a small number of observations. It was quite surprising to find that the removal of *only two successive outlying points from the B curve* can change the situation dramatically, see Fig. 17. The lower curve is the evaluation of the

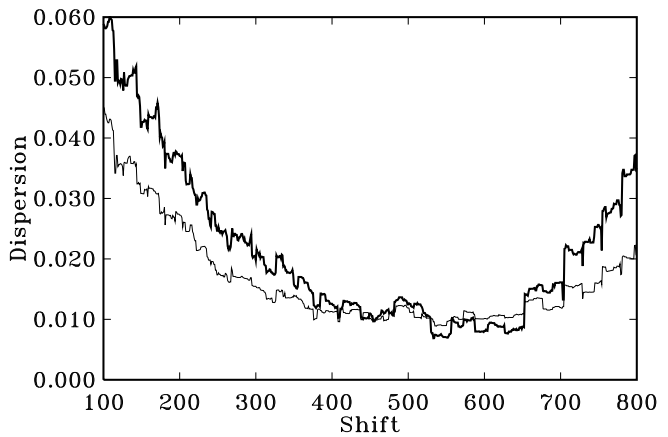


**Fig. 14.** Dispersion spectra for the original radio data sets. The bold curve is  $D_{A,B}^2(\tau)$  and the normal curve is  $D_{all}^2(\tau)$ .

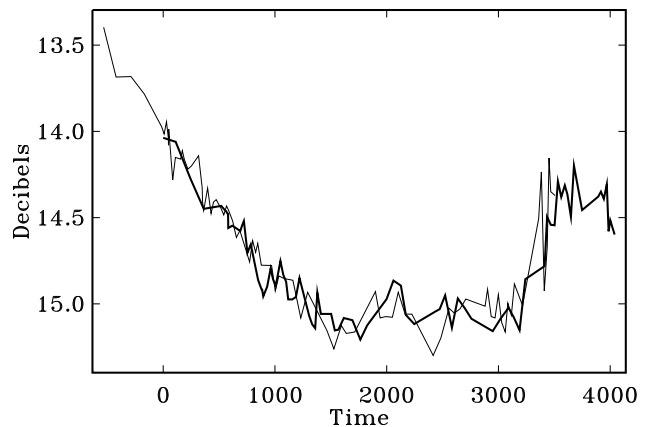


**Fig. 15.** Radio data sets combined for the best shift and parameter  $a$ . The bold curve is A, the normal curve is shifted B data.

$\tau = 536$  days hypothesis against the  $\tau = 415$  days hypothesis, when removing pairs of observations from *only the B curve*. The upper curve depicts the same statistic for the data with two points removed from the B data set (the skipped points are from April 10, 1990 and May 7, 1990). It is seen that the data set with skips in the B curve is relatively stable against further removing of time points. In Fig. 18 the original data points for the A and B curve are depicted, with linear interpolation between the points. The “bad” points are exactly the points which cause the strong fluctuation at the very end of the B data set.

We proceed now with data set B without the two “bad” points. It is no surprise to see that the main minimum of the  $D_{A,B}^2$  spectrum moves to  $\tau = 409$  days and that the overall correspondence between the artificial spectrum and the real one is also good (see Fig. 19). Quite pleasing is also the plot of the optimally shifted B curve with two skipped points and the original A curve (see Fig. 20).

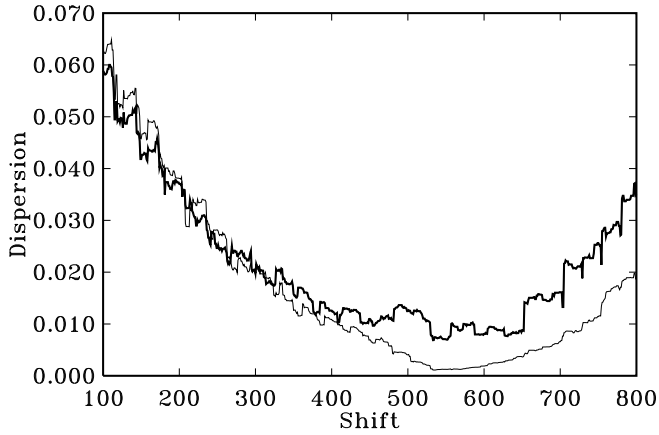


**Fig. 16.** Comparison of the dispersion spectra for the original radio and artificial data sets. The bold curve is  $D_{A,B}^2(\tau)$  for the original radio data, the normal curve is  $D_{A,B}^2(\tau)$  for the artificial data.

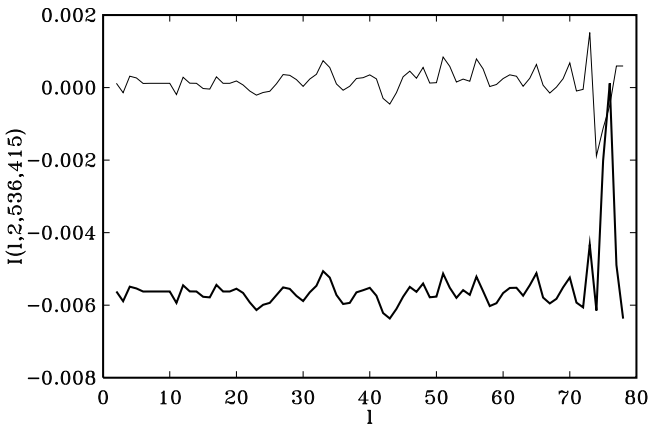


**Fig. 17.** Effect of data skipping to  $D_{A,B}^2(536) - D_{A,B}^2(415)$ . The bold curve depicts the gain (Eq. 7) computed for the original radio data sets. The normal curve depicts the gain computed for the radio data with two skipped outlying points from B curve.

Bootstrapping gives us an error of  $\pm 23$  days for the shift, thus the correspondence between the results obtained from the optical and the radio observations is rather good. The error value must not be taken too seriously, since the use of a 7-point median filtering to build the mean curve estimates is somewhat arbitrary. However, it can be understood as a reasonable guess.

#### 4. Discussion

Let us first take the original optical and radio data sets as they are. We were able to reproduce the results of the rather complex analysis in PRHa and PRHb, using extremely simple statistics. However, the simple formulation

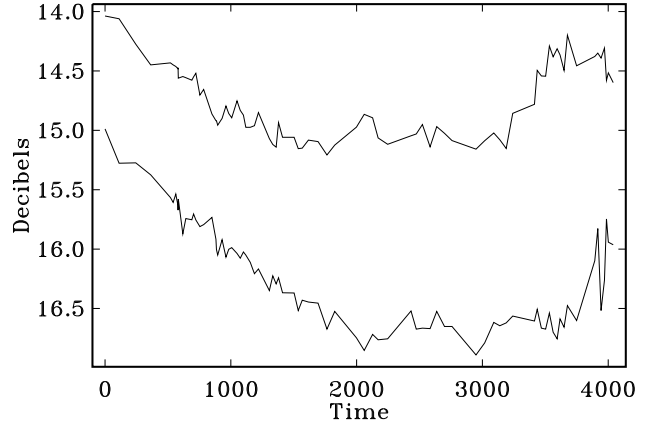


**Fig. 18.** Linearly interpolated observations of the A and B curve. The upper curve is B, the lower curve is A.

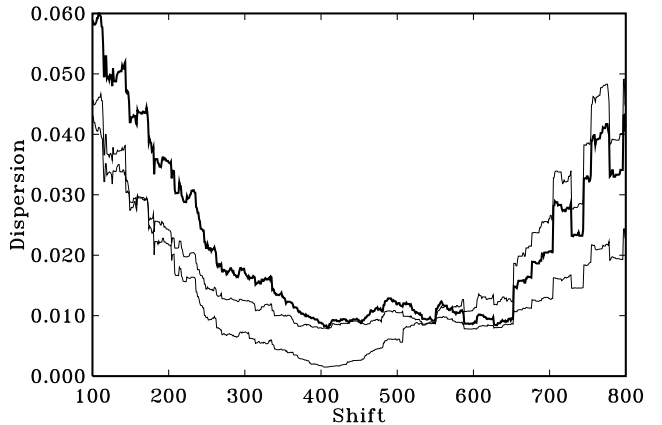


**Fig. 19.** Dispersion spectra for the radio data sets with skipped two time points from B curve. The bold curve is  $D_{A,B}^2(\tau)$ , the flat normal curve is  $D_{all}^2(\tau)$  for radio data with skips, the steeper normal curve is the corresponding dispersion for artificial data.

of our procedures also allowed to get additional insights into what is actually going on. We now summarize the *pro* and *contra* arguments.

##### 4.1. Contra $\tau = 536$ days

The feature around  $\tau = 536$  days is located near the absolute minimum of the window function in the optical dispersion spectra and does not have a profile which is expected from the artificial curves. *There is a large excess for the dispersion in the overlapped regions of the shifted light curves, and this is revealed using both methods of analysis.* The last fact also invalidates the Monte-Carlo results in PRHa because their data set models are too regular compared to the real data sets. This is well illustrated in Fig.

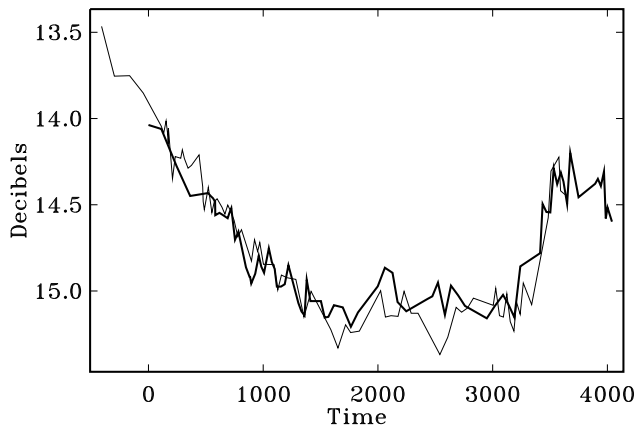


**Fig. 20.** Optimally shifted radio observations with two skips in B curve. The bold curve depicts A data and the normal curve shifted B data.

2. The dispersion spectra in the 536 days region are rather sensitive to skipping few data points and detrending.

#### 4.2. Pro $\tau = 536$ days

Original data sets are used. The statistically sound optimal prediction method and simple explorative type analysis method give essentially the same results. No additional or excessively metaphysical arguments are involved in the data analysis. Good correspondence between optical and radio results.

#### 4.3. Contra $\tau = 415$ days

The good looking results are obtained after somewhat arbitrary detrending and removing part of the data from analysis. From the purist's point of view this is unacceptable.

#### 4.4. Pro $\tau = 415$ days

For both data sets the results of the explorative analysis are relatively consistent and stable. The dispersion for the overlapped region in the spectrum for the optical data is nearly the same as for other regions. The overall form of the depressions in the dispersion spectra mimic quite well model spectra.

#### 4.5. Future work

After the first version of this paper was completed a more extensive optical data set became available to us. These data have been obtained by R. Schild and contain 707 time points from November 1979 to June 1993. Here we present only a very short analysis of the new data, details will be presented elsewhere. In Fig. 21 the dispersion spectrum for the full data set *without any detrending and without*

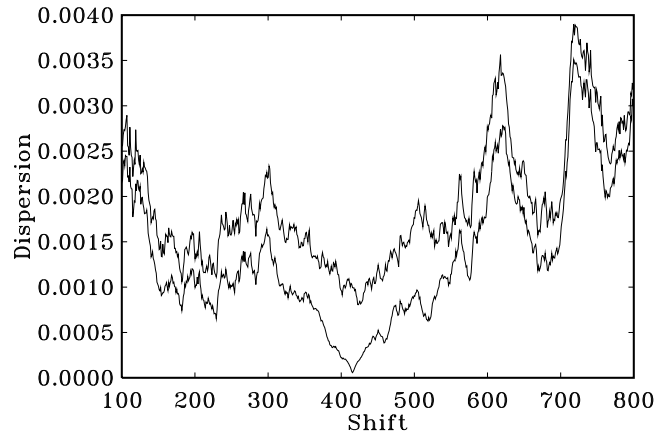


**Fig. 21.** Dispersion spectra for the extended data set provided to us by R. Schild. The upper curve is  $D_{A,B}^2(\tau)$ , the lower curve is  $D_{A,B}^2(\tau)$  for the corresponding artificial data set with time shift  $\tau = 415$  days.

*any skips* is plotted against the spectrum of the artificial data set which was computed by 7-point median filtering of the coalesced original data (with B curve shifted by 415 days). It can be seen that the feature around 536 days is practically absent and the depression around 415 days is well pronounced. This result is in good agreement with the analysis made by Schild and Thomson (1993) and Thomson and Schild (1993).

The number of observations in the extended data set is now much larger and probably sufficient to address the rather complicated question about the statistical significance of the feature around 415 days. As we demonstrated in Section 2 the straightforward Monte-Carlo modelling can lead us to a wrong conclusion. Therefore we plan to use more complex waveform models for the data sets which will include also parts describing microlensing.

## 5. Conclusions

We introduced an extremely simple, but nevertheless sensitive method to seek probable time delay values for light curves which are assumed to originate from one and the same source. The method easily recovered results which were obtained by more complex and statistically sound procedures presented in PRHa and PRHb. However, the simplicity of the proposed method allowed us to get additional insights into the problems which originate from unfortunate spacing of the sampling points for the optical light curves. It allowed us also to produce an alternative consistent solution for the time delay problem.

The dispersion spectra of the optical and radio data can show minima in various places depending on the method of analysis and preprocessing of the data. For theoretical reasons delays  $\tau \leq 0$  can be excluded. The minimum near 1.5 years most probably results from a statis-

tical fluctuation which is amplified due to the windowing, since for this time shift the overlap of data from the two light curves is at a minimum and thus the least squares minimization has more freedom to fit free parameters.

For the radio data we found that removing only two observations from B gives a stable spectrum for the dispersions, with a best value for the shift near  $\tau = 409$  days. This result is in good agreement with the value of  $\tau = 415$  days for the optical curve, which reveals itself after the detrending of the original data, or in other circumstances which allow to depress the instable minimum around 536 days.

We think that the time delay controversy on QSO 0957+561 A,B is still not settled, but there is quite strong evidence (especially if we take into account preliminary results obtained using the extended data set by R. Schild) that the time delay is in the region of 400-420 days.

*Acknowledgements.* We wish to thank L. Nieser, P. King and A. Dent for helpful discussions and computational aid. It is a pleasure to acknowledge valuable discussion with Rudy Schild and David Thomson, who also kindly provided us with their unpublished data. We finally appreciate the comments and constructive criticism on the first version of this paper by an anonymous referee. Part of this work was supported by the *Deutsche Forschungsgemeinschaft, DFG* under Re 439, Schr 417 and 436 EST.

## A. Appendix. Nonparametric dispersion estimates

### A.1. Dispersion estimation through subsampling

For a set of variables  $y_i, i = 1, 2, \dots, N$  we observe that

$$\begin{aligned} & \frac{1}{2N^2} \sum_{i=1}^N \sum_{j=1}^N (y_i - y_j)^2 = \\ &= \frac{1}{2N^2} \sum_{i=1}^N \sum_{j=1}^N ((y_i - \mu) - (y_j - \mu))^2 = \\ &= \frac{1}{N} \sum_{i=1}^N (y_i - \mu)^2 - \frac{1}{N^2} \left( \sum_{i=1}^N (y_i - \mu) \right)^2. \end{aligned} \quad (\text{A1})$$

If we set  $\mu = \frac{1}{N} \sum_{i=1}^N y_i$  the second term in the last expression vanishes and consequently the first double sum can be considered as a standard (slightly biased) estimator for the sample dispersion. Taking into account that  $(y_i - y_j)^2 = (y_j - y_i)^2$  and using another normalization we can obtain the standard unbiased estimate  $S^2$  for the dispersion:

$$\begin{aligned} S^2 &= \frac{1}{N(N-1)} \sum_{i=1}^{N-1} \sum_{j=i+1}^N (y_i - y_j)^2 = \\ &= \frac{1}{N-1} \sum_{i=1}^N (y_i - \mu)^2. \end{aligned} \quad (\text{A2})$$

Let  $K = N(N-1)/2$  be the total number of squares in the first sum, so that:

$$S^2 = \frac{1}{K} \sum_{k=1}^K \frac{(y_{i(k)} - y_{j(k)})^2}{2} = \frac{1}{K} \sum_{k=1}^K d_k. \quad (\text{A3})$$

The sequence of half squares  $d_k = (y_{i(k)} - y_{j(k)})^2/2$  can be looked upon as a general finite sample from which we can draw random subsamples  $d_{k(l)}, l = 1, 2, \dots, L$ . In this case the mean values

$$\hat{S}^2 = \frac{1}{L} \sum_{l=1}^L d_{k(l)} \quad (\text{A4})$$

approximate the original estimate  $S^2$ . How good are these approximations? From standard sampling theory (Cochran 1964) we get the estimate for the dispersion of  $\hat{S}^2$  (*subsampling dispersion*):

$$\mathbf{D}(\hat{S}^2) = \mathbf{E}(\hat{S}^2 - \mathbf{E}\hat{S}^2) = \frac{(K-L)D^2}{KL}, \quad (\text{A5})$$

where  $\mathbf{E}$  is mathematical expectation operator,  $D^2$  is the dispersion for the full sample of half squares

$$D^2 = \frac{\sum_{k=1}^K (d_k - \bar{d})^2}{K-1}, \quad (\text{A6})$$

and  $\bar{d}$  is their mean value. We see that the approximation error vanishes if  $L$  approaches  $K$ . The important point is that even for small values of  $L$  the subsampling error is as small as  $D^2/L$ .

For the particular case of normally distributed  $y_i$ s the half squares are distributed according to the scaled  $\chi^2(1)$  law and consequently  $D^2$  can be substituted by the value of  $2\sigma^2$  where  $\sigma$  is the standard deviation for the  $y_i$  or some of its estimates.

Putting now all things together we get the main result of this paragraph: the dispersion  $S^2$  can be estimated as *half sum of squares chosen randomly from the full set*. The approximate dispersion of this estimate can generally be computed from any available estimate of the original dispersion of  $y_i$ , and in particular from  $\hat{S}^2$  itself:

$$\mathbf{D}(\hat{S}^2) = \frac{2(K-L)\hat{S}^2}{KL}. \quad (\text{A7})$$

Of course, for a simple estimation of the dispersion, our scheme is rather cumbersome, but as we will see later, it can be very useful in more complicated situations. In mathematical statistics the estimates of type (A2) are known as *U-statistics* (Hoeffding, 1948) and estimates based on subsampling as *incomplete U-statistics* (Blom, 1976).

### A.2. Trend as nuisance

Let us now consider the regression model

$$y_i = g(t_i) + \epsilon_i = g_i + \epsilon_i, i = 1, 2, \dots, N, \quad (\text{A8})$$

where the  $t_i$  are randomly distributed time points,  $g(t)$  is some smooth but unknown function of time (trend), the  $y_i$  are observed values and the  $\epsilon_i$  are unknown observational errors. We are seeking an estimate for the dispersion of the  $\epsilon_i$ .

Normally the trend  $g(t)$  is approximated by some parametric model and estimates for the  $\epsilon_i$  and also for their dispersion are computed from residuals after some fitting procedure. But, as demonstrated below, the estimate for the dispersion can be computed without knowing the exact form of  $g(t)$ .

Let us first write down the general dispersion of the observed values

$$\begin{aligned} S_{\text{obs}}^2 &= \frac{1}{N(N-1)} \sum_{i=1}^{N-1} \sum_{j=i+1}^N (y_i - y_j)^2 = \\ &= \frac{1}{N(N-1)} \sum_{i=1}^{N-1} \sum_{j=i+1}^N ((e_i - e_j) + (g_i - g_j))^2 = \\ &= S_{\text{err}}^2 + S_{\text{trend}}^2 \\ &\quad + \frac{2}{N(N-1)} \sum_{i=1}^{N-1} \sum_{j=i+1}^N (e_i - e_j)(g_i - g_j). \end{aligned} \quad (\text{A9})$$

The last sum can be considered as small (at least for samples containing enough observations) since trend and error are not correlated. The value for the trend dispersion  $S_{\text{trend}}^2$  can, however, be significant. In order to get an estimate for the error dispersion  $S_{\text{err}}^2$  we must somehow eliminate the trend dispersion from the general sum. From the discussion above we know that we are not forced to use all pairs of squares to get dispersion estimates. Let us choose only those pairs which have close enough observing times. Formally we can define a *selection window*

$$G(\delta, t_i, t_j) = \begin{cases} 1 & |t_i - t_j| \leq \delta \\ 0 & \text{otherwise} \end{cases} \quad (\text{A10})$$

for some specified maximum allowable lag  $\delta$ , and enter it into the general sum

$$\hat{S}^2(\delta) = \frac{1}{2} \frac{\sum_{i=1}^{N-1} \sum_{j=i+1}^N G(\delta, t_i, t_j) (y_i - y_j)^2}{\sum_{i=1}^{N-1} \sum_{j=i+1}^N G(\delta, t_i, t_j)}. \quad (\text{A11})$$

This choice of a subsample from the total of squares is not random from the point of view of its construction, but it is random from the point of view of the statistics of errors.

For a slowly varying trend  $g(t)$  we can assume that it is Lipschitz continuous with some maximum slope parameter  $A$

$$|g(t_i) - g(t_j)| \leq A|t_i - t_j| \quad (\text{A12})$$

and consequently the upper limit for the dispersion of the trend part can be estimated by

$$\begin{aligned} &\frac{1}{2} \frac{\sum_{i=1}^{N-1} \sum_{j=i+1}^N G(\delta, t_i, t_j) (g_i - g_j)^2}{\sum_{i=1}^{N-1} \sum_{j=i+1}^N G(\delta, t_i, t_j)} \leq \\ &\leq \frac{1}{2} \frac{\sum_{i=1}^{N-1} \sum_{j=i+1}^N G(\delta, t_i, t_j) A^2 (t_i - t_j)^2}{\sum_{i=1}^{N-1} \sum_{j=i+1}^N G(\delta, t_i, t_j)} \leq \\ &\leq \frac{1}{2} (A\delta)^2 \end{aligned} \quad (\text{A13})$$

The last limit is quite conservative, so that it should be used only for rather crude guesses. Fortunately, the second sum can also be computed from the time point sequence.

For every fixed value of  $\delta$  there are

$$L = \sum_{i=1}^{N-1} \sum_{j=i+1}^N G(\delta, t_i, t_j) \quad (\text{A14})$$

pairs of squares to be taken into account when estimating the dispersion. The error from subsampling increases with decreasing  $L$  (and of course with decreasing  $\delta$ ). But the bias due to the trend part of the observed values (*modelling error*) decreases with decreasing  $\delta$ . Consequently there is a certain value for  $\delta$  where both errors are of comparable magnitude. Let us call this tradeoff value *optimal* (see Fig. 4). The corresponding  $\hat{S}^2(\delta)$  can be used as an estimate for the original error dispersion.

There is another well known procedure to choose a subsample of squared differences. We can select only pairs which consists of neighbouring observations in the original data. The corresponding estimate for dispersion is now

$$\hat{S}^2 = \frac{1}{2(N-1)} \sum_{i=1}^{N-1} (y_i - y_{i+1})^2. \quad (\text{A15})$$

In this estimate we avoided introduction of any free parameters into the selection scheme. Similar estimates were proposed by different authors (see von Neumann et al. 1941 or in the context of periodicity search Lafler&Kinman 1965).

It is also possible to combine two subsampling schemes given above. In this case only neighbouring pairs of observations  $y_i, y_j$  for which  $|t_i - t_j| \leq \delta$  are included into the subsample. Thereby we avoid additional scatter in our estimates due to the *long gaps* in the data set. However, every additional restriction for selected pairs decreases their total number and consequently increases the subsampling error.

## References

- Cabrera-Caño J., Alfaro E. J., Polvorinos A., 1990, in: Errors, bias and uncertainties in astronomy, eds. C. Jaschek and F. Murtagh, Cambridge University Press., p. 101
- Beskin G.M., Oknyanskij V.L., 1992, Lect. Not. Phys. 406, 67

- Blom G., 1976, *Biometrika* 63, 573
- Borgeest U., 1986, *AJ* 309, 467
- Cochran W.G., 1964, *Sampling Techniques* 2nd edn., Wiley, New York
- Falco E.E., Wambsganss J., Schneider P., 1991a, *MNRAS* 251, 698
- Falco E.E., Gorenstein M.V., Shapiro I.I., 1991b, *ApJ* 372, 364
- Falco E.E., 1992, *Lect. Not. Phys.* 406, 50
- Florentin-Nielsen R., 1984, *A&A* 138, L19
- Gondhalekar P.M., Wilson R., Dupree A.K., Burke B.F., 1986, in: *London Conference Proceedings "New Insights in Astrophysics: Eight Years of Astronomy with IUE"* SP-263, p. 715
- Gorenstein M.V., Bonometti R.J., Cohen N.L., Falco E.E., Shapiro I.I., Bartel N., Rogers A.E.E., Marcaide J.M., Clark T.A., 1988, *Proc. IAU Symp.* 129, 201
- Hoeffding W., 1948, *Ann. Math. Stat.* 19, 293
- Lafler J., Kinman T.D., 1965, *ApJS* 11, 216
- Lehár J., Hewitt J.N., Roberts D.H., 1989, *Lect. Not. Phys.* 330, 84
- Lehár J., Hewitt J. N., Roberts D. H., Burke B. F., 1992, *ApJ* 384, 453
- von Neumann J., Kent R.H., Bellinson B.I., Hart B.I., 1941, *Annals of Math. Stat.* 12, 153
- Press W.H., Rybicki G.B., Hewitt J.N., 1992a, *ApJ* 385, 404 (PRHa)
- Press W.H., Rybicki G.B., Hewitt J.N., 1992b, *ApJ* 385, 416 (PRHb)
- Refsdal S., 1964a, *MNRAS* 128, 295
- Refsdal S., 1964b, *MNRAS* 128, 307
- Roberts D.H., Lehár J., Hewitt J. N., Burke B.F., 1991, *Nature* 352, 43
- Rybicki G.B., Press H.W., 1992, *ApJ* 398, 169
- Schild R., Choffin B., 1986, *ApJ* 300, 209
- Schild R.E., 1990, *Lect. Not. Phys.* 360, 102
- Schild R.E., Thomson D.J., 1993, *Proceedings of the 31h Liège International Astrophysical Colloquium, June 21-25, 1993*, in press.
- Thomson D.J., Schild R.E., 1993, *Proceedings of the International Conference on Applications of Time Series Analysis in Astronomy and Meteorology, September 6-10, 1993*, Padua, preprint.
- Vanderriest C., Schneider J., Herpe G., Chevretton M., Moles M., Wlérick G., 1989, *A&A* 215, 1
- Vanderriest C., Gosset E., Remy, M., Swings, J.-P., 1992, *Lect. Not. Phys.* 406, 107
- Walsh D., Carswell R.F., Weymann R.J., 1979, *Nature* 279, 381
- Young P., 1980, *ApJ* 241, 507

